

VENTRICULAR FUNCTION

Rapid Assessment of Left Ventricular Segmental Wall Motion, Ejection Fraction, and Volumes with Single Breath-Hold, Multi-Slice TrueFISP MR Imaging

David S. Fieno, PhD, MD,¹ Louise E.J. Thomson, MB ChB, FRACP,¹ Piotr J. Slomka, PhD,^{1,2} Aiden Abidov, MD, PhD,¹ Hidetaka Nishina, MD,¹ Daisy Chien, PhD,¹ Sean W. Hayes, MD,¹ Rola Saouaf, MD,¹ Guido Germano, PhD, MBA,¹ John D. Friedman, MD, FACC,^{1,2} and Daniel S. Berman, MD, FACC,^{1,2}

¹Departments of Imaging and Medicine (Division of Cardiology), and CSMC Burns & Allen Research Institute, Cedars-Sinai Medical Center, Los Angeles, California, USA

²Department of Medicine, University of California Los Angeles, School of Medicine, Los Angeles, California, USA

ABSTRACT

Background and Objective: To reduce imaging time and complexity, we sought to determine whether single breath-hold, multi-slice TrueFISP (SB-MST) magnetic resonance imaging (MRI) method is comparable to standard multi-breath-hold, multi-slice TrueFISP (MB-MST) for assessment of left ventricular (LV) wall motion abnormality (WMA), volumes, and ejection fraction (EF). **Methods and Results:** We studied 62 patients having cardiac MRI at 1.5-Tesla. After acquiring standard MB-MST (one slice per breath-hold), SB-MST was performed, acquiring 3 short- and 2 long-axis views over only 20 heartbeats. Using both techniques, wall motion was scored using a 6-point, 17-segment LV model for all scans (62 patients × 2 techniques/patient = 124 scans) on two separate occasions. Separately, EF and ventricular volumes were evaluated using both MB-MST and SB-MST. For all analyses, MB-MST was considered the standard against which SB-MST was compared. Twenty-six of 62 patients exhibited at least one segmental WMA by MB-MST. Exact agreement for wall motion was found in 965/1054 segments (92%, kappa = 0.74, p < 0.001), and agreement was within 1 score point in 1010/1054 segments (96%). Considering a score >1 abnormal, exact agreement for presence of WMA was found in 131/193 segments (68%) abnormal by MB-MST and for absence of WMA in 838/861 segments (97%) normal by MB-MST. Agreement within 1 score point occurred in 167/193 abnormal (87%) and in 843/861 normal segments (98%). There were no significant differences in agreement between first and second read of the data. Variability of SB-MST on read one versus read two was small (5%, 996/1054 segments read identically, p = ns) and statistically identical to variability of MB-MST on read one versus read two (4%, 1007/1054 segments read identically, p = ns). For end-diastolic volumes, end-systolic volumes, and EF using SB-MST compared to MB-MST, mean differences were 9 ± 15 ml, 6 ± 12 ml, and 2 ± 5%, and correlations were r = 0.97, 0.98 and 0.95, respectively. **Conclusion:** SB-MST accurately assesses wall motion, volumes and EF. This approach may serve as a screening exam for assessment of WMA and, under select circumstances, may substitute for standard multi-breath-hold method in situations requiring rapid accurate assessments of LV function.

Keywords: Left Ventricular Wall Motion, Ventricular Volumes, Ejection Fraction, Cardiac Magnetic Resonance, Rapid Imaging.

Correspondence to:

Daniel S. Berman, MD, FACC

Cedars-Sinai Medical Center,

8700 Beverly Boulevard, Room A-041

Los Angeles, California 90048

tel: (310) 423-4223 fax: (310) 423-0811

e-mail: bermand@cshs.org

INTRODUCTION

Accurate identification of segmental wall motion abnormality (WMA) and determination left ventricular volumes and ejection fraction (EF) are important for management and serial assessment of patients with known or suspected cardiac disease. WMA at rest, during exercise or with pharmacological stress is strongly suggestive of underlying coronary artery disease (CAD) and is used routinely for noninvasive diagnosis (1–3). For several

decades, EF has been the most important clinical descriptor of global left ventricular function (4).

In recent years, magnetic resonance imaging (MRI) has become widely accepted as a gold standard for assessment of WMA, ventricular volumes, and EF (5, 6). A true tomographic method with high spatial and temporal resolution, MRI has favorable signal to noise characteristics, ability to derive images in any desired orientation, and strongly correlates with other imaging methods (6–8). After initial validation with spin echo acquisitions requiring prolonged acquisitions, faster cine MRI methods became routinely applied. At the present time true fast imaging with steady-state precession (TrueFISP) has become a routine acquisition method on clinical MRI scanners (9), and multiple breath-hold multiple slice TrueFISP has become the standard image acquisition approach for purposes of assessment of ventricular function (10).

While faster than the previous cine methods, multiple breath-holds over a few minutes are still standard practice with conventional implementation of the TrueFISP method. In a typical protocol, patients hold their breath for 10 to 20 seconds per slice, with 10 to 15 short-axis and 2 to 4 long-axis slices acquired, resulting in 10 to 20 separate breath-holds for a given cine examination (11). Given the marked increase in signal-to-noise with TrueFISP over previous techniques, we reasoned that this approach might be used to reduce imaging time by reducing resolution, while still accurately measuring ventricular function. In previous work others have employed real-time approaches with some success for determination of regional WMA, ventricular volumes, and ejection fraction (10–18). In the present study, we evaluated the utility of a fast imaging technique in which a cine image of a single slice with 20-phases can be acquired in four to five heartbeats (19). Using this method, overall image quality is improved versus that of real-time methods but the short acquisition time of the method allows for multiple slices in a single breath-hold. The hypothesis of this study was that a single breath-hold, multi-slice TrueFISP (SB-MST) MRI technique would allow accurate assessment of left ventricular WMA, volumes, and EF in comparison to the standard multiple breath-hold multiple slice TrueFISP (MB-MST) method.

MATERIALS AND METHODS

We consecutively enrolled patients ($n = 62$) undergoing cardiac MRI for clinical purposes or as part of a research protocol. All examinations performed were in compliance with the Institutional Review Board at our medical center and all enrolled patients signed informed consent.

Imaging

Patients were studied on a clinical 1.5-Tesla MR scanner (Siemens Sonata, Erlangen, Germany). Following scout images to determine the short- and long-axes of the heart, standard MB-MST cine images were acquired using a retrospectively ECG-gated sequence covering all ventricular slices in the short axis as well as mid two- and four-chamber slice, acquired in

standard fashion, ie, one slice per breath hold (10, 11). Each view was acquired in a single breath-hold, requiring 12 heart beats (9 to 14 seconds in duration depending on heart rate). Imaging parameters were as follows: field-of-view 350×270 – 350 mm; matrix 256×192 – 256 (depending on patient size); temporal resolution 45 msec; slice thickness 8 mm; slice gap 2 mm; TE/TR 1.6/3.1 msec; pixel bandwidth 930 kHz; flip angle 60° ; and 20 phases/cardiac cycle; and segment size 5 to 9 lines, depending on heart rate. Following the MB-MST imaging, the SB-MST method was used to acquire 3 short-axis (distal, mid, and basal) and two long axis (mid two- and four-chamber) cine images in a single breath-hold. This sequence reduces total imaging time by reducing the number of frequency encoding steps by 50% and by using an interpolation algorithm in k-space to share phases across the cardiac cycle (19). Field-of-view, slice thickness, echo/repetition time, phases and slice positioning were identical to those acquired during individual breath-holds. The SB-MST sequence differed from MB-MST in the following parameters: matrix (128×108 – 128 depending on patient size), temporal resolution (60 msec), pixel bandwidth (1300 kHz), flip angle (58°), segment size (11 to 16 lines depending on heart rate), and number of heartbeats over which data were acquired (20, breath-hold duration 16 to 24 seconds, depending on heart rate).

Wall motion analysis

For the analysis of wall motion, patient images were randomized and read by consensus of observers (LEJT, AA, JDF, DSB for read one; HN and DSF for read two) on two separate occasions separated in time by >6 months where readers were blinded to patient identity, pulse sequence used, and results of previous reads. Semiquantitative segmental wall motion scores were assigned values between 0 to 5, where 0 = normal, 1 = mild hypokinesis, 2 = moderate hypokinesis, 3 = severe hypokinesis, 4 = akinesis, and 5 = dyskinesis, using a 17-segment model of the left ventricle (LV). For each image sequence, the same five-slice cine images were viewed (distal, mid, and basal short axis, and mid 2- and 4-chamber long axis). Image quality was also judged for each study as being excellent, good, fair, or poor. Comparison of segmental wall motion score between the two cine imaging techniques was made based on agreement of segment-by-segment score, which was considered exact when scores were identical, close when the scores differed by 1 point, and lack of agreement was considered present when the segmental score differed by ≥ 2 points. The proportion of concordantly normal and concordantly abnormal segments by the two imaging methods was also assessed; for this purpose, scores of 0 and 1 were grouped, and only scores ≥ 2 were considered abnormal, consistent with standard clinical practice. The overall degree of myocardial dysfunction was assessed by comparing the total number of dysfunctional segments/patient and the number of normal segments/patient as well as by comparing the global summed wall motion score obtained by simple summation of the 17 segment scores/patient with each method. Values for the first and second reads of each technique (MB-MST and SB-MST)

were compared to determine variability between different reads. All data for the second read were re-analyzed and concordance of normal and abnormal segments between MB-MST and SB-MST was compared to the first read.

Ventricular volume and EF analysis

For the analysis of ventricular volumes and EF from MB-MST, values were computed by manually outlining endocardial borders at end-diastole and end-systole of all short axis slices containing the left ventricular cavity using a clinical workstation (Argus, Siemens Medical Systems, Erlangen, Germany) as previously described (20). Selection of end-systole and end-diastole was based on visual identification of the images with the smallest and largest chamber diameter, respectively. The manually assigned contours were checked by a second observer (DSF) for each patient to assure accuracy in delineation of each border and when necessary the borders were redrawn. Papillary muscles were considered as belonging to the LV chamber volumes. End-diastolic and end-systolic volumes (EDV and ESV, respectively) were computed using a modified Simpson's rule (6, 21), taking into account pixel size and slice spacing.

Since the standard clinical workstation does not allow calculation of volumes and EF from a combination of slices acquired in multiple orientations (long-axis, short axis), for SB-MST, LV volumes and EF were separately computed using a newly developed software package (Quantitative Magnetic Resonance,

QMR, Cedars-Sinai Medical Center, Los Angeles, CA) which provides this functionality (22). To compute LV volumes and EF, two additional observers (AA, PS) blinded to the results of the MB-MST analysis manually created contours of the two-chamber and four-chamber long axis views at end-diastole and end-systole, with frame selection based on visual assessment of chamber size, similar to above analysis. Two-dimensional (2D) image contours were transformed to three-dimensional (3D) image space exploiting relative image orientation information of vertical and horizontal long-axis images contained in the header files. Subsequently, a 3D LV surface was derived from the software by automatically creating interpolated multiple 2D contours placed between the LV base and apex. These contours were visualized as they occurred on three short-axis slices and further adjusted manually in these planes using four control points and smoothly change in the radial dimension. Each contour was then fitted to four 3D points placed by the user on two- and four-chamber views. These contours were constrained to pass through all four points and smoothly change in the radial dimension. The valve plane was fitted separately in 3D to the last four points obtained from both long-axis views (see Fig. 1). Using the 3D model, LV volumes at end-diastole and end-systole were computed and used to determine EFs.

Statistical methods

Agreement for wall motion score between SB-MST and MB-MST was assessed using a kappa statistic. Linear regression and

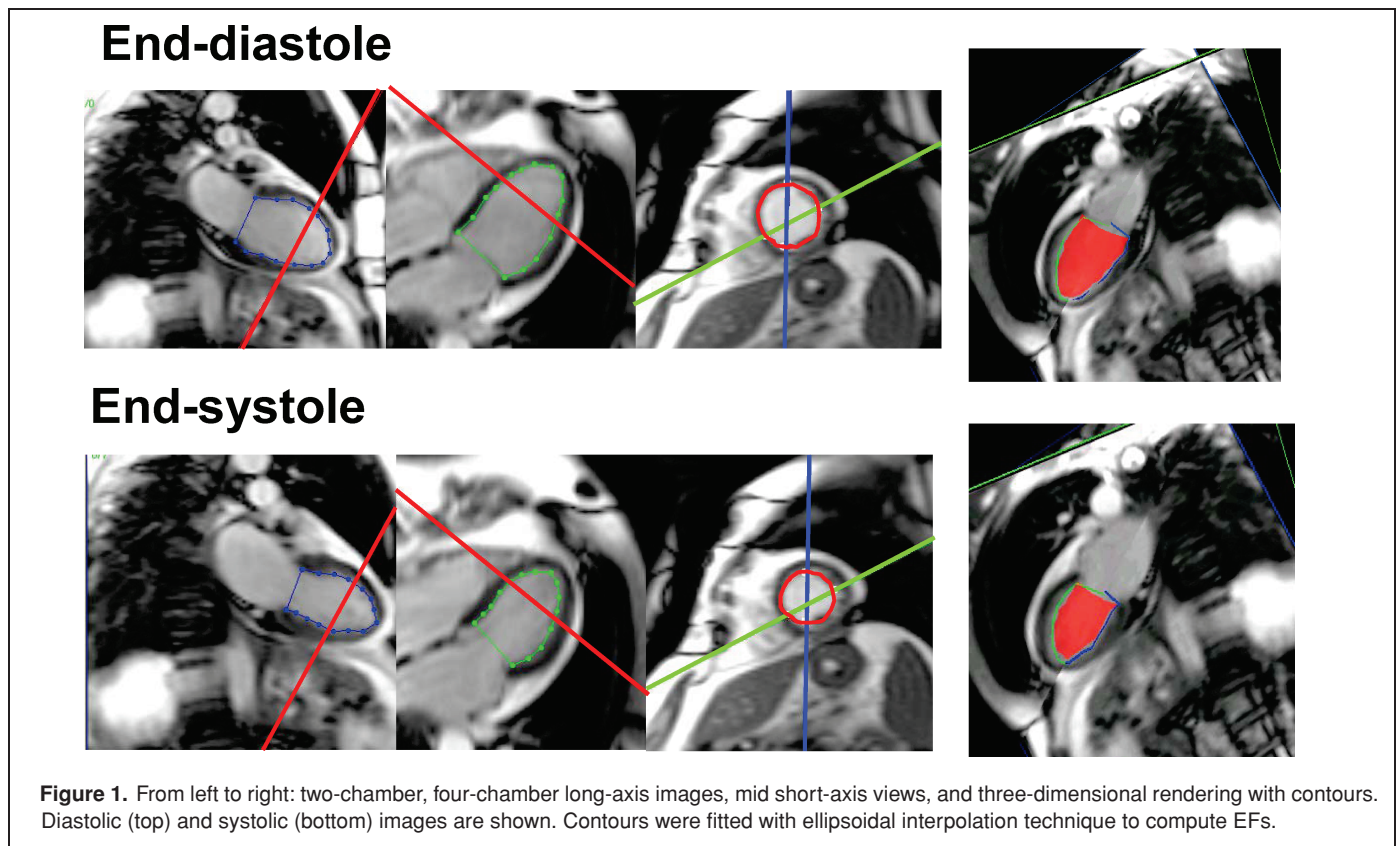


Table 1. Characteristics of the study population

Parameter	Males (n = 45)	Females (n = 18)	Overall (n = 62)
Age	67 ± 16	68 ± 13	67 ± 15
Prior MI	7	2	9
Prior CABG	3	10	13
Prior PCI	8	6	14
Prior Angiogram ¹	15	10	25
Suspected CAD ²	11	7	18
Cardiomyopathy ³	2	2	4
Valvular Disease ⁴	2	1	3
End Diastolic Volume, mL ⁵	175 ± 65*	114 ± 58	149 ± 68
Ejection Fraction, % ⁵	52 ± 17*	60 ± 13	55 ± 16
# Dysfunctional Segs ⁵	4 ± 6	2 ± 4	3 ± 5
Breath-holds ⁶	13 ± 2*	11 ± 1	12 ± 2

Abbreviations: MI = myocardial infarction; CABG = coronary artery bypass grafting; PCI = percutaneous coronary intervention; CAD = coronary artery disease; Dysf Segs = dysfunctional segments.

*Indicates that $p < 0.05$ for difference between males and females.

¹Indicates that patient underwent a prior angiogram demonstrating at least one coronary artery with $>50\%$ stenosis.

²Indicates that coronary artery disease was highly suspected based positive stress test but never demonstrated by angiography.

³Indicates that patient had a nonischemic cardiomyopathy.

⁴Indicates that patient had severe valvular disease documented by echocardiography.

⁵Indicates the value determined using standard MB-MST imaging.

⁶Indicates the number required for MB-MST imaging in all short- and long-axis views.

Bland-Altman analyses were employed to determine whether systematic differences existed between methods for ventricular volumes and EF (23). Values were expressed as mean ± standard deviation. Differences between men and women in the study population were assessed using two-tailed Fisher's Test. Differences between the two MRI examinations were compared using a student's paired t-test where a p-value of less than 0.05 was considered significant.

RESULTS

Clinical characteristics of the study population, mean quantitative parameters, and number of dysfunctional segments determined are shown in Table 1. By MB-MST, 26/62 patients demonstrated ≥ 1 segmental WMA, EF was $55 \pm 16\%$ (range 16 to 81%, 19/62 with EF $< 50\%$). For MB-MST, an average of 12 ± 2 breath-holds were required to cover the heart.

Figure 2 shows images from a patient acquired using MB-MST and SB-MST techniques. In all patients, SB-MST was acquired in a single breath-hold on the first attempt and all images were considered technically adequate for assessment of WMA, ventricular volumes, and EF. In comparison to MB-MST, SB-MST provided greater ventricular coverage (1 vs 5 slices/breath-hold, respectively) but poorer spatial resolution (1.2 vs 2.4 mm in-plane, respectively), and required more heartbeats to acquire (12 vs 20 heartbeats, respectively). Regarding image quality, 53 of 62 SB-MST studies (85%) were judged to be ex-

cellent (8 good, 1 fair) and 48/62 MB-MST data sets (77%) were judged to be excellent (14 good, 1 fair) ($p = ns$).

Segmental wall motion scores in a total of 1054 segments (62 patients \times 17 segments per patient) comparing SB-MST and MB-MST are shown in Table 2. Exact segmental agreement was seen in 965/1054 segments (92%, kappa = 0.74). Agreement within 1 wall motion score was found in 1010/1054 (96%). When the analysis was limited to segments considered to have WMA (scores ≥ 2), exact segmental score agreement was seen in 131/193 segments (68%), and agreement within 1 score was found in 167/193 (87%). Importantly, of the 193 segments considered abnormal by MB-MST, 171 (89%) were abnormal by SB-MST, while 842/861 segments (98%) normal by MB-MST were found to be normal by SB-MST.

There were 44/1054 segments (4 %) with scores differing by ≥ 2 . Of these, the largest group (39/44 segments, 89%) were characterized as normal by one of the methods and found to be at least moderately abnormal by the other approach. Interestingly, these points came from 16/62 patients studied and, while the overall population had 3 ± 5 dysfunctional segments (See Table 1), patients in this group had 7 ± 6 dysfunctional segments ($p < 0.05$). Furthermore, there were similar numbers of segments judged to have ≥ 2 higher score by each method (24 by SB-MST and 20 by MB-MST).

Excellent agreement was found for the extent of ventricular dysfunction by the two methods. The summed wall motion score comparisons between SB-MST and MB-MST are illustrated in Figure 3. Table 3 shows the overall extent of ventricular dysfunction/patient by each method. Of the 32 patients identified by MB-MST as having a WMA, 31 also had a WMA by SB-MST and agreement within 1 segment was observed in 28. Of the 30 patients with no WMA by MB-MST, 28 had no WMA by SB-MST.

Inter- and intra-study variability of the above results was calculated following a second read of both the MB-MST and SB-MST data sets by separate observers. When SB-MST was compared to MB-MST on a second read, results were as follows: number of patients with ≥ 1 segmental WMA by MB-MST 25/62 ($p = ns$, one patient was different between reads), exact segmental agreement in 1020/1054 segments (97%) between MB-MST reads, segmental agreement within 1 score in 1044/1054 segments (99%) between SB-MST and MB-MST ($p = ns$ for difference between reads), exact agreement of SB-MST for segments judged abnormal by MB-MST in 172/196 segments ($p = ns$ compared to first read), exact agreement of SB-MST for segments judged normal by MB-MST in 848/858 segments ($p = ns$ compared to first read), and summed wall motion score correlation line was $y = 0.97 \times + 0.1$ ($r = 0.98$) with bias and limits of agreement 0.2 ± 1.3 for SB-MST versus MB-MST ($p = ns$ for both compared to first read).

Results of the comparison of volumes and EF using SB-MST and MB-MST are shown in Figure 4. For EDV, ESV, and EF, correlation coefficients were $r = 0.97$, 0.98 and 0.95 , respectively, the slopes were near unity for each measurement (95% confidence intervals were (0.90–1.03), (0.93–1.04), and (0.86–1.03)), and the y-intercept was close to zero (95% confidence

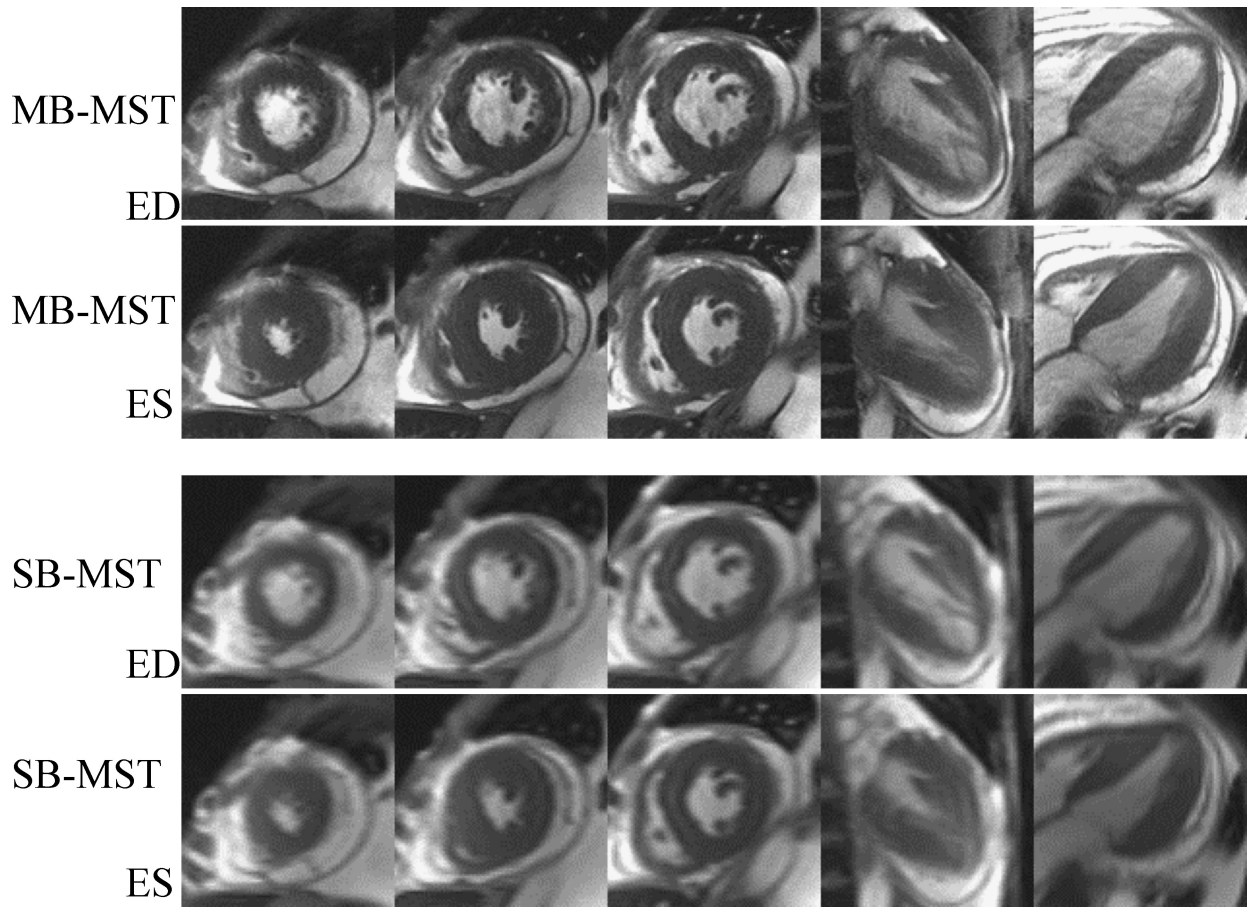


Figure 2. Comparison between standard multiple breath-hold multi-slice TrueFISP (MB-MST, top two rows) and single breath-hold multi-slice TrueFISP (SB-MST, bottom two rows) cine acquisition at diastole (1st and 3rd rows) and systole (2nd and 4th rows). In this patient, the mid and basal short-axis slices were judged to have anterolateral wall motion abnormalities with identical scoring for the single and multiple breath-hold techniques.

intervals were (4.3–22.0), (2.5–11.9), (–3.8–5.6), respectively). Bland-Altman analysis revealed mean differences were 9 ± 15 ml, 6 ± 12 ml, and $2 \pm 5\%$, respectively. When patients with $EF < 50\%$ ($n = 19$) were those with normal EF ($n = 43$), the bias and limits of agreement of the two groups were $3 \pm 5\%$ and $3 \pm 5\%$, respectively ($p = ns$ between normal and abnormal).

DISCUSSION

Cardiac MRI has become the ‘gold standard’ for determination of EF and ventricular volumes as well as characterization of regional myocardial function (6, 9, 24), assessments which are central to the evaluation of the cardiac patient. Virtually all of the cardiac MRI imaging techniques for obtaining these parameters, however, are performed over multiple minutes, and characteristically require several consecutive breath holds. There has been some success with real-time approaches but these images can suffer from poor overall quality, motion artifacts, or both (10, 12–18). To our knowledge, this is a first study

to describe and validate a non real-time, single breath, multi-slice cine cardiac MRI method for assessment of LV EF, volumes, and segmental wall motion in a clinical population of 62 patients.

Table 2. Segmental score agreement between SB-MST and MB-MST for visual semi-quantitative assessment of wall motion

SB-MST	MB-MST						Totals
	5	4	3	2	1	0	
5	18	2	2	0	0	0	22
4	1	21	7	0	0	0	29
3	2	8	65	2	1	3	81
2	0	0	16	27	3	14	60
1	0	0	0	0	0	2	2
0	0	0	4	18	4	834	870
Totals	27	31	94	47	8	852	1054

Exact agreement 92%, kappa = 0.74, $p < 0.0001$.

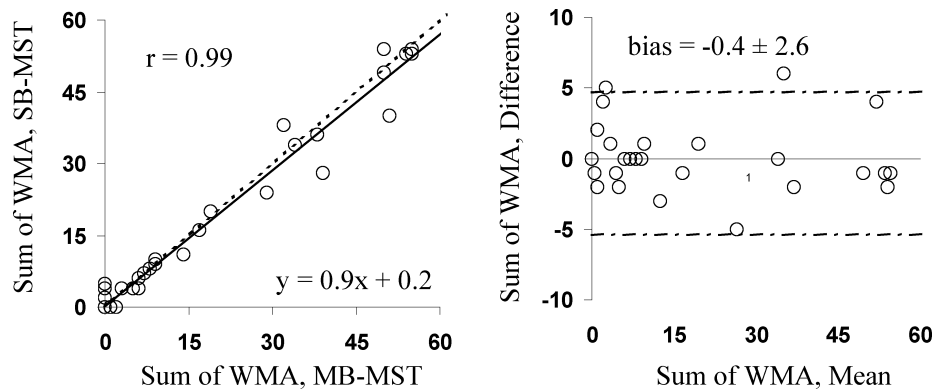


Figure 3. Plot demonstrating the relationship between summed wall motion abnormality (WMA) score per patient using MB-MST (x-axis) versus SB-MST (y-axis). Dotted line represents the line of identity; solid line represents the regression equation. Corresponding Bland-Altman plot is also shown for summed WMA score. Dashed lines represent positive and negative limits of agreement.

Characterization of function using CMR

Despite the robustness of cardiac MRI in patients with heart disease, challenges come with the actual determination of WMA extent and measurement of volumes and EF in routine clinical practice. The goal of high image quality has resulted in a standard method of acquiring one slice per breath-hold and, hence, multiple individual breath-holds are necessary for a complete examination. Since this approach requires several minutes for acquisition of all slices, it is not practical in circumstances where rapid imaging is needed. Such a requirement is already being noted in circumstances such as dobutamine stress, in which a complete image set during the peak of stress would be desirable. Furthermore, data suggest that differences in diaphragmatic position during repeated breath-holding may be associated with slice misregistration during three-dimensional analyses (25), which could lead to errors in quantification of volumes and EF. In addition, multiple breath-holds may be tiring for some patients, particularly individuals with poor LV function and/or co-morbidities. Finally, the standard approach for assessment of EF and ventricular volumes requires endocardial contouring at diastole and

systole for each slice position—a process that is relatively time consuming and has potential for error (26). Thus, despite the image quality and robust identification of cardiac anatomy with standard, multiple breath-hold techniques, motivation exists to explore faster, easier methods for evaluation of myocardial systolic function (10, 27).

Several strategies have evolved for reducing acquisition times during MR scans. Real-time cardiac cine images acquire fewer k-space lines using sequences with short repetition times to minimize overall imaging time and reconstruct images that are not acquired over several cardiac cycles. Kaji et al. (10) described such an approach in which patients ($n = 14$) were free breathing during imaging and reported good correlations with EF, ventricular volumes, and ventricular mass when compared to standard approaches acquiring one slice per breath hold. Similarly, Lee and colleagues (11) studied 20 subjects using real-time and segmented TrueFISP and found good agreement for ventricular parameters computed using the accelerated and standard approaches. Setser et al. studied a real-time echo planar pulse sequence in volunteers ($n = 10$) and also found strong correlation between real-time and standard approaches (28), as have a several other groups working in this area (13, 15, 17, 18, 29). However, real-time approaches have practical disadvantages in that signal-to-noise and temporal resolution are greatly reduced compared to segmented approaches, and these effects are amplified when artifacts are present in images.

A different strategy is to use segmented techniques with reduced k-space requirements to reduce acquisition times, instead of real-time imaging. Parallel imaging, phase sharing, and partial Fourier methods implement this concept and represent a compromise between the speed of real-time and the quality of standard segmented approaches (27, 30–32). In this study, we utilize this latter approach, which allowed us imaging during one breath-hold to evaluate LV function in three short- and two long-axis views.

The SB-MST technique examined in the present study showed favorable characteristics with regard to image quality (Fig.1), produced similar values of qualitative wall motion

Table 3. Total number of dysfunctional segments per patient assessed by SB-MST and MB-MST

SB-MST	MB-MST								Totals	
	≥8	7	6	5	4	3	2	1		0
≥8	12	0	0	0	0	0	0	0	0	12
7	0	0	0	0	0	0	0	0	0	0
6	0	0	1	0	0	0	0	0	0	1
5	0	0	0	1	0	0	0	0	0	1
4	0	0	0	1	0	0	0	0	0	1
3	0	0	0	0	0	2	0	1	0	3
2	0	0	0	0	0	1	5	0	1	7
1	0	0	0	0	0	0	1	6	1	8
0	0	0	0	0	0	0	0	1	28	29
Totals	12	0	1	2	0	3	6	8	30	62

Exact agreement 92%, kappa = 0.84, $p < 0.0001$.

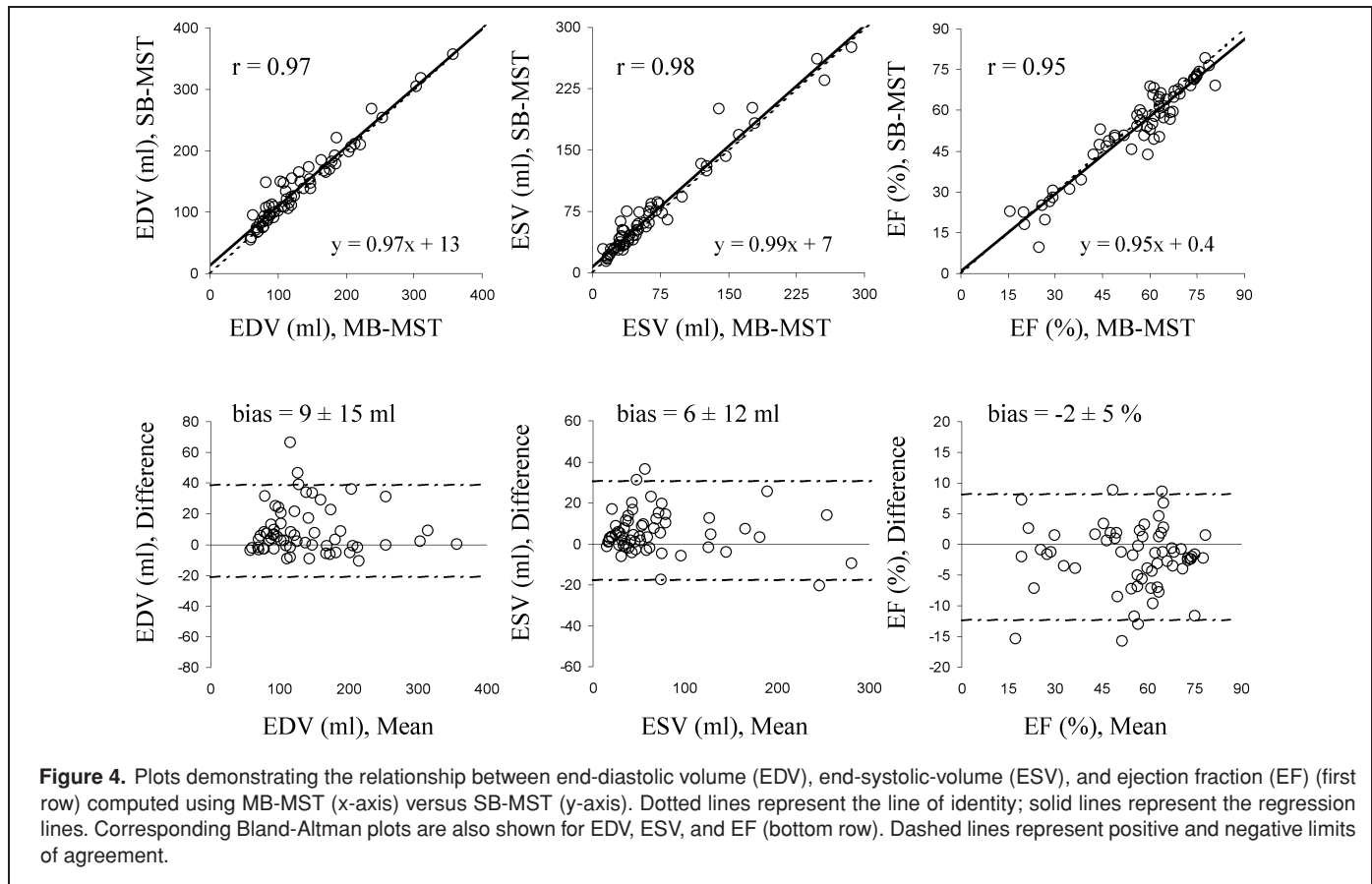


(Table 2) and ventricular volumes (Fig. 5), and was performed in a single, 20-heartbeat breath-hold in all 62 patients. In addition, by computing ventricular volumes and EF from two long-axis and three short-axis slices using SB-MST, the number of contours that had to be manually drawn on the images was reduced in comparison to that required to contour the entire short-axis stack using MB-MST.

Regarding assessment of segmental wall motion abnormality, close correspondence between the methods was also found. Exact segmental agreement was noted in 92% of segments. When confined to segments with WMA by the MB-MST method, 89% of segments were also abnormal by SB-MST, and there was an agreement within one score in 87% of segments. Of importance, when the segmental score was substantially different by the methods, there were similar numbers of segments showing a greater degree of abnormality by each technique, and these discrepancies were seen predominantly in a small subgroup with extensive regional dysfunction. These findings suggest that the main discordance was related to visual variation in segmental assignment in individual patients rather than to differences between the methods. This suggestion is supported by the analysis of the summed wall motion score (Fig. 4), which demonstrated a correlation coefficient of 0.99 with close correspondence throughout the range of wall motion abnormalities. The findings confirm that the rapid SB-MST method is effective for assessment of regional dysfunction. In addition, the measure-

ments of EDV, ESV, and EF by SB-MST highly correlated with those of the standard MB-MST technique. Given the ease with which these measurements are made, the technique of using two long axis images with three short-axis slices as opposed to the full complement of the short axis data might be useful for obtaining these measurements even if standard imaging methods are used; ie, since the two long axis sequences that were used for these computations with the SB-MST method are routinely acquired in most circumstances where the MB-MST acquisitions are being performed, the approach we have defined for measurement of EDV, ESV, and EF may be applicable beyond the SB-MST acquisitions.

In principle, there may be advantages of incorporating long-axis information in 3D calculations of ventricular volume. Analysis of long-axis images in this study greatly aided in delineation of the apex and the mitral valve plane, which are known to be sources of potential error when analyzing stacks of short-axis images (33). The SB-MST technique in the present study may have application to at least two clinical settings. First, one may be able to assess regional wall motion and global EF in a single breath-hold, rather than the average 12 ± 2 (see Table 1) required for the MB-MST. This would reduce both imaging time and time required to analyze images, and potentially make examination by MRI easier for patients unable or unwilling to perform multiple similar breath-holds. Second, a fast imaging technique with a sampling of the entire myocardium in multiple views may

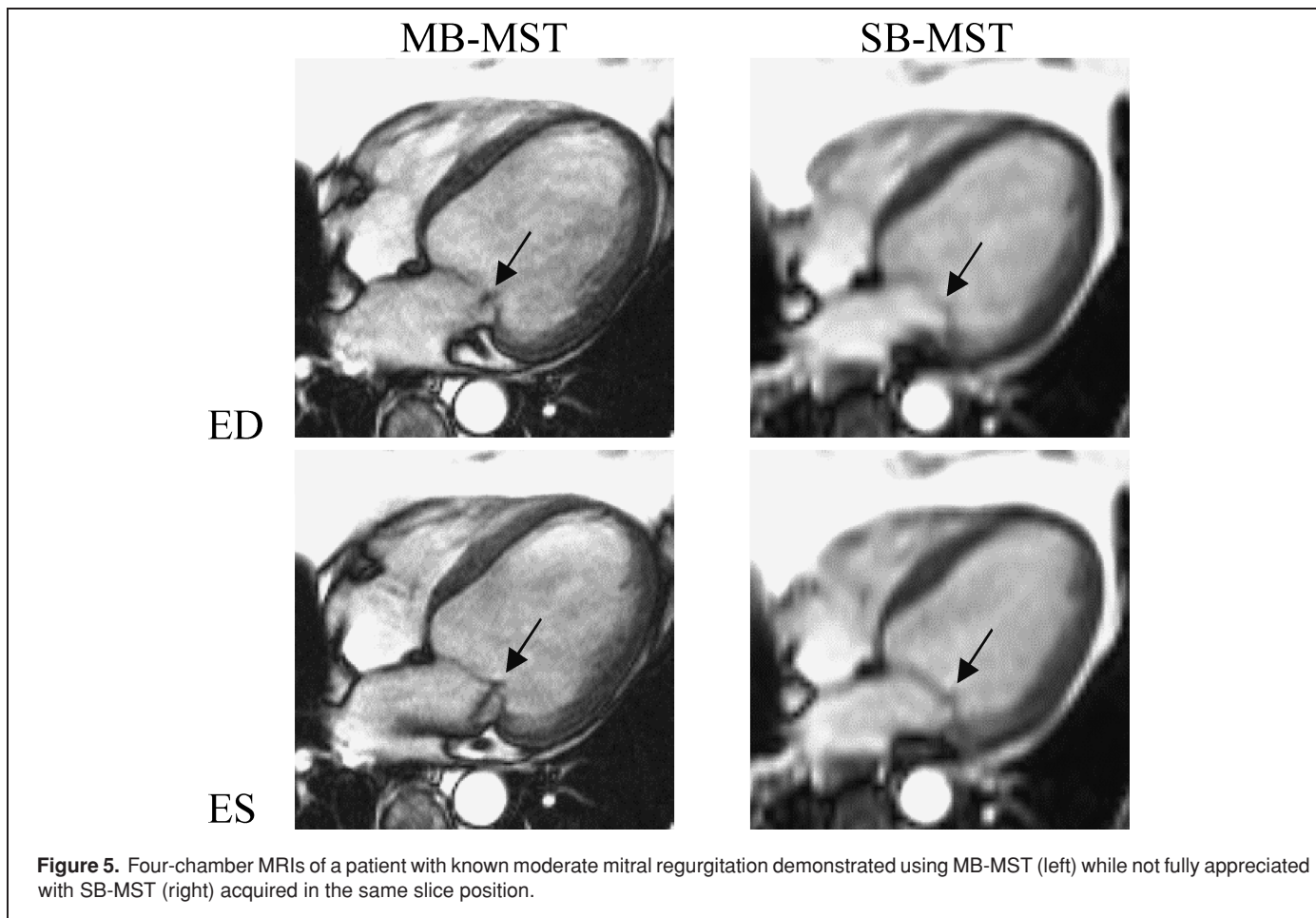


Figure 5. Four-chamber MRIs of a patient with known moderate mitral regurgitation demonstrated using MB-MST (left) while not fully appreciated with SB-MST (right) acquired in the same slice position.

be applicable to settings where fast assessment of wall function, ventricular volumes, and EF is desired at rest and during some form of increased myocardial demand, ie, stress testing. In addition, it may be that multi-slice single breath-hold imaging reduces errors related to slice misregistration across multiple breath-holds. Exploration of these applications in patients undergoing MR examination may be warranted.

Study limitations

While the data of the present study are encouraging, it may be that a single breath-hold technique such as the one examined in this study introduces new challenges. For example, in this method, careful selection of the distal, mid, and basal short-axis as well as accurate prescription of the long-axis views are necessary to ensure accurate depiction of the myocardium for analysis in the 17-segment model. While this was possible in our patient population, it may present challenges in patients with abnormal ventricular geometry and for centers that do not do a high volume of cardiac MRI. In addition SB-MST required collection of data over 20 heartbeats, whereas MB-MST required 12 heartbeats per acquisition. Often, patients were hyperventilated for the multi-slice technique to facilitate the extended breath-hold. Also, the SB-MST as it is presented in the current study may fail at high

heart rates due to poor overall temporal resolution. Although this issue could be potentially offset by allowing for additional heart beats, longer breath holds, and/or imaging over additional breath holds, it is unclear whether patients would tolerate these changes necessary for acquisition of higher temporal resolution data. It should also be noted that turbulent flow from valvular regurgitation was less evident on SB-MST in 6 patients with known moderate to severe mitral insufficiency as opposed to MB-MST acquired in the same orientations. An example of one patient with mitral insufficiency imaged using both techniques is shown in Figure 5. This incidental observation suggests that standard cine imaging techniques may be superior to faster acquisitions for evaluation of valvular disease, although the data of the present study do not formally address this topic.

An assumption of the calculation of the EF from the sampled views is that the shape of the ventricle should approximate a prolate ellipsoid (34). In the current study, few patients had marked deformation of the left ventricular shape in which this assumption would not hold. The degree to which the method will be accurate in patients with severe alteration of ventricular shape will require further study. In our study, although 19/62 patients had EF <50%, mean EF was 55% and, therefore, the applicability of the method used for EF determination still needs to be evaluated in a large series. In fact, our study had less than 1/3 of patients,

overall, with abnormal EFs and therefore the current method may only be useful as a screen. In determination of WMA, we noted that a larger percentage of abnormal segments were judged differently by SB-MST than normal segments (68% versus 98% with exact agreement, respectively) versus MB-MST. It remains to be determined how accurate SB-MST is in large populations with abnormal ventricular function.

CONCLUSION

A single breath-hold, multi-slice TrueFISP technique can provide assessments of LV segmental wall motion, volumes and EF, which correlate closely with those determined using the standard techniques requiring several breath-holds. This new approach may serve as a useful screening tool for wall motion and, in select circumstances, may substitute for MB-MST in clinical situations where rapid accurate assessments of ventricular function and volumes are required.

ABBREVIATIONS

CAD Coronary Artery Disease
 MRI Magnetic Resonance Imaging
 WMA Wall Motion Abnormality
 ED End-Diastole
 ES End-Systole
 TrueFISP True Fast Imaging with Steady-State Precession
 SB-MST Single Breath-Hold Multi-Slice TrueFISP
 MB-MST Multiple Breath-Hold Multi-Slice TrueFISP
 DICOM Digital Imaging and Communication in Medicine

ACKNOWLEDGMENTS

The authors would like to gratefully acknowledge Edward Gill, BS, RT (MR), John LaMarche, CRT (MR), Laura Smith, BS, RT (MR), and Mark Golden BS, RT (MR) for their assistance with the MRI examinations, as well as Allison Hamilton, BS, for her outstanding help as a study coordinator.

REFERENCES

- Rozanski A, Diamond GA, Jones R, Forrester JS, Berman D, Morris D, Pollock BH, Freeman M, Swan HJ. A format for integrating the interpretation of exercise ejection fraction and wall motion and its application in identifying equivocal responses. *J Am Coll Cardiol* 1985;5:238–48.
- Williams MJ, Marwick TH, O’Gorman D, Foale RA. Comparison of exercise echocardiography with an exercise score to diagnose coronary artery disease in women. *Am J Cardiol* 1994;74:435–8.
- Nagel E, Lehmkuhl HB, Bocksch W, Klein C, Vogel U, Frantz E, Ellmer A, Dreyse S, Fleck E. Noninvasive diagnosis of ischemia-induced wall motion abnormalities with the use of high-dose dobutamine stress MRI: comparison with dobutamine stress echocardiography. *Circulation* 1999;99:763–70.
- Parameshwar J, Keegan J, Sparrow J, Sutton GC, Poole-Wilson PA. Predictors of prognosis in severe chronic heart failure. *Am Heart J* 1992;123:421–6.
- Pattynama PM, De Roos A, Van der Wall EE, Van Voorthuisen AE. Evaluation of cardiac function with magnetic resonance imaging. *Am Heart J* 1994;128:595–607.
- Ioannidis JP, Trikalinos TA, Dianas PG. Electrocardiogram-gated single-photon emission computed tomography versus cardiac magnetic resonance imaging for the assessment of left ventricular volumes and ejection fraction: a meta-analysis. *J Am Coll Cardiol* 2002;39:2059–68.
- Perrone-Filardi P, Bacharach SL, Dilsizian V, Maurea S, Marin-Neto JA, Arrighi JA, Frank JA, Bonow RO. Metabolic evidence of viable myocardium in regions with reduced wall thickness and absent wall thickening in patients with chronic ischemic left ventricular dysfunction. *J Am Coll Cardiol* 1992;20:161–8.
- Chuang ML, Hibberd MG, Salton CJ, Beaudin RA, Riley MF, Parker RA, Douglas PS, Manning WJ. Importance of imaging method over imaging modality in noninvasive determination of left ventricular volumes and ejection fraction: assessment by two- and three-dimensional echocardiography and magnetic resonance imaging. *J Am Coll Cardiol* 2000;35:477–84.
- Carr JC, Simonetti O, Bundy J, Li D, Pereles S, Finn JP. Cine MR angiography of the heart with segmented true fast imaging with steady-state precession. *Radiology* 2001;219:828–34.
- Kaji S, Yang PC, Kerr AB, Tang WH, Meyer CH, Macovski A, Pauly JM, Nishimura DG, Hu BS. Rapid evaluation of left ventricular volume and mass without breath-holding using real-time interactive cardiac magnetic resonance imaging system. *J Am Coll Cardiol* 2001;38:527–33.
- Lee VS, Resnick D, Bundy JM, Simonetti OP, Lee P, Weinreb JC. Cardiac function: MR evaluation in one breath hold with real-time true fast imaging with steady-state precession. *Radiology* 2002;222:835–42.
- Hori Y, Yamada N, Higashi M, Hirai N, Nakatani S. Rapid evaluation of right and left ventricular function and mass using real-time true-FISP cine MR imaging without breath-hold: comparison with segmented true-FISP cine MR imaging with breath-hold. *J Cardiovasc Magn Reson* 2003;5:439–50.
- Plein S, Smith WH, Ridgway JP, Kassner A, Beacock DJ, Bloomer TN, Sivananthan MU. Measurements of left ventricular dimensions using real-time acquisition in cardiac magnetic resonance imaging: comparison with conventional gradient echo imaging. *Magma* 2001;13:101–8.
- Lamb HJ, Doornbos J, van der Velde EA, Kruit MC, Reiber JH, de Roos A. Echo planar MRI of the heart on a standard system: validation of measurements of left ventricular function and mass. *J Comput Assist Tomogr* 1996;20:942–9.
- Schalla S, Nagel E, Lehmkuhl H, Klein C, Bornstedt A, Schnackenburg B, Schneider U, Fleck E. Comparison of magnetic resonance real-time imaging of left ventricular function with conventional magnetic resonance imaging and echocardiography. *Am J Cardiol* 2001;87:95–9.
- Hunter GJ, Hamberg LM, Weisskoff RM, Halpern EF, Brady TJ. Measurement of stroke volume and cardiac output within a single breath hold with echo-planar MR imaging. *J Magn Reson Imaging* 1994;4:51–8.
- Plein S, Smith WH, Ridgway JP, Kassner A, Beacock DJ, Bloomer TN, Sivananthan MU. Qualitative and quantitative analysis of regional left ventricular wall dynamics using real-time magnetic resonance imaging: comparison with conventional breath-hold gradient echo acquisition in volunteers and patients. *J Magn Reson Imaging* 2001;14:23–30.
- Nayak KS, Pauly JM, Nishimura DG, Hu BS. Rapid ventricular assessment using real-time interactive multislice MRI. *Magn Reson Med* 2001;45:371–5.
- Larson AC, Simonetti OP. A comparison of rectilinear reduced field of view TrueFISP cine imaging techniques (abstract). Proceedings of the 3rd Annual Meeting of the Society of Cardiovascular Magnetic Resonance (SCMR). Atlanta, GA, January 21–23, 2000.

20. Kim RJ, Wu E, Rafael A, Chen EL, Parker MA, Simonetti O, Klocke FJ, Bonow RO, Judd RM. The use of contrast-enhanced magnetic resonance imaging to identify reversible myocardial dysfunction. *N Engl J Med* 2000;343:1445–53.
21. Fieno DS, Hillenbrand HB, Rehwald WG, Harris KR, Decker RS, Parker MA, Klocke FJ, Kim RJ, Judd RM. Infarct resorption, compensatory hypertrophy, and differing patterns of ventricular remodeling following myocardial infarctions of varying size. *J Am Coll Cardiol* 2004;43:2124–31.
22. Slomka P, Mehta T, Aladi UE, Berman DS, Germano G. A fully automated registration-based technique for segmentation of the left ventricle from cardiac MRI. Proceedings of the 4th Annual Meeting of the Society of Cardiovascular Magnetic Resonance, 2004.
23. Bland JM, Altman DG. Statistical methods for assessing agreement between two methods of clinical measurement. *Lancet* 1986;1:307–10.
24. Hundley WG, Morgan TM, Neagle CM, Hamilton CA, Rerkpattanapit P, Link KM. Magnetic resonance imaging determination of cardiac prognosis. *Circulation* 2002;106:2328–33.
25. Shea SM, Kroeker RM, Deshpande V, Laub G, Zheng J, Finn JP, Li D. Coronary artery imaging: 3D segmented k-space data acquisition with multiple breath-holds and real-time slab following. *J Magn Reson Imaging* 2001;13:301–7.
26. Francois CJ, Fieno DS, Shors SM, Finn JP. Left ventricular mass: manual and automatic segmentation of true FISP and FLASH cine MR images in dogs and pigs. *Radiology* 2004;230:389–95.
27. Rehwald WG, Kim RJ, Simonetti OP, Laub G, Judd RM. Theory of high-speed MR imaging of the human heart with the selective line acquisition mode. *Radiology* 2001;220:540–7.
28. Setser RM, Fischer SE, Lorenz CH. Quantification of left ventricular function with magnetic resonance images acquired in real time. *J Magn Reson Imaging* 2000;12:430–8.
29. Bornstedt A, Nagel E, Schalla S, Schnackenburg B, Klein C, Fleck E. Multi-slice dynamic imaging: complete functional cardiac MR examination within 15 seconds. *J Magn Reson Imaging* 2001;14:300–5.
30. Weiger M, Pruessmann KP, Boesiger P. Cardiac real-time imaging using SENSE. SENSitivity Encoding scheme. *Magn Reson Med* 2000;43:177–84.
31. Sodickson DK, Manning WJ. Simultaneous acquisition of spatial harmonics (SMASH): fast imaging with radiofrequency coil arrays. *Magn Reson Med* 1997;38:591–603.
32. Kozerke S, Tsao J, Razavi R, Boesiger P. Accelerating cardiac cine 3D imaging using k-t BLAST. *Magn Reson Med* 2004;52:19–26.
33. Young AA, Axel L. Three-dimensional motion and deformation of the heart wall: estimation with spatial modulation of magnetization—a model-based approach. *Radiology* 1992;185:241–7.
34. Dodge HT, Sheehan FH. Quantitative contrast angiography for assessment of ventricular performance in heart disease. *J Am Coll Cardiol* 1983;1:73–81.